

Research on dynamic micro-deformation under laser point source

X.F. Wang^{a,b,c,*}, G.N. Chen^b, Sh.G. Hu^a, J. Takacs^c, Gy. Krallics^c, Y.P. Su^a

^a*School of Mechanical Engineering and Automation, Beijing University of Aeronautics and Astronautics, 37 Xueyuan Road, Haidian District, Beijing 100083, Peoples's Republic of China*

^b*Institute of Mechanics, Chinese Academy of Science, Beijing 100080, Peoples's Republic of China*

^c*Budapest University of Technology and Economics, Hungary*

Received 24 June 2004; accepted 20 January 2005

Available online 9 April 2005

Abstract

The dynamic micro-deformation of the specimen under laser point source is measured using a laser beam reflex amplifier system and numerically simulated by Msc.Marc software. Compared with experimental result and calculated result, the final deformation direction of the specimen depends on the result of the thermal strain and the phase transformation strain cooperation, away from the laser beam or towards the laser beam, the final deformation angle depends on temperature gradient in the thickness direction and the geometry constraint of the specimen. The conclusion lays the foundation for further research on the mechanism of laser bending. At the same time, it is proposed that the model of calculation based on classical Fourier heat transfer theory cannot be enough to simulate the dynamic micro-deformation of the specimen under laser point source, the model of calculation should be modified in the future.

© 2005 Elsevier Ltd. All rights reserved.

Keywords: Dynamic micro-deformation process; Laser bending; Numerical simulation

1. Introduction

Laser processing is an advanced and high efficiency manufacturing method and has very wide applied perspective in aviation, mechanical engineering and industry of nation defense and so on. Laser bending is a flexible processing method that combines laser technique with metal forming technique. It has a characteristic of making sheet metal deform without dies and is suitable for not only bending the small batch components, but also bending high variation and special shape, miniature dimension, large simple components difficult in processing. It also can correct large complex workpiece precisely. So application of laser bending has a good prospect for producing prototypes in aviation and space flight, apparatus and sample car. There is a lot of research work done in laser

bending principle [1–4], numerical simulation of laser bending process [4–8], effect factors and change regularities of laser bending process [4,9–17]. Due to lack of research on laser bending mechanisms, the value and direction of deformation cannot be controlled so that its application fields can be confined only to a certain extent. According to the laser bending process it is that laser point source moves along the irradiation line, so the final deformation of sheet metal is produced under heat accumulation. The dynamic micro-deformation process is researched under laser point source in order to understand the mechanism of laser bending better.

This paper research on dynamic micro-deformation of the specimen under laser point source through experiment and calculation interacted verification. The dynamic micro-deformation of the specimen under laser point source is measured using a laser beam reflex amplifier system and numerically simulated by Msc.Marc software. Compared with experimental result and calculated result, the final deformation direction of the specimen depends on the result of the thermal strain and the phase transformation strain cooperation, away from the laser beam or towards the laser beam, the final deformation angle depends on temperature gradient in the thickness direction and the geometry

* Corresponding author. Address: School of Mechanical Engineering and Automation, Beijing University of Aeronautics and Astronautics, 37 Xueyuan Road, Haidian District, Beijing 100083, Peoples's Republic of China. Tel.: +86 10 8231 7704/8231 5495; fax: +86 10 8231 7735.

E-mail address: wangxiufeng@buaa.edu.cn (X.F. Wang).

constraint of the specimen. The conclusion lays the foundation for further research on the mechanism of laser bending. At the same time, it is proposed that the model of calculation based on classical Fourier heat transfer theory cannot be enough to simulate the dynamic micro-deformation of the specimen under laser point source, the model of calculation should be modified in the future.

2. Experiment

2.1. Experimental method

The experiment has been done in the Faculty of Transportation Engineering, Budapest University of Technology and Economics. The scheme of the experiment for research on the dynamic micro-deformation process is shown in Fig. 1.

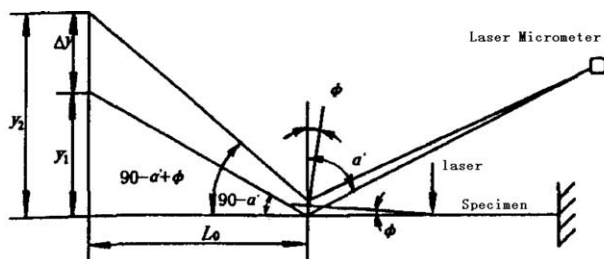
A 1800 W CO₂ laser is used in the continuous wave (CW) mode, its power density distribution is TEM₀₀. The wavelength of the laser beam is 10.6 μm, and the focus length of lens is 5". The laser beam is guided through an optical fiber cable from the controller to the laser beam head. An on/off switch, the output power, the heating time of the laser beam and the movement of the x–y table are controlled by a CNC program. The CNC control

unit accuracy is 0.005 mm. Materials St14 and C45 (100 mm×2 mm×2 mm) are chosen. The specimen is clamped at one end as a cantilever beam and put at 21 mm under the focal point of lens (beam diameter on the specimen surface is 2 mm). The specimen is irradiated on its middle by the laser beam, the laser output power is 100 W and the continued heating time is 0.782 s. The specimen surface is sprayed with a graphite coating (Graphite 33) in order to enhance absorption of the laser energy. A small piece of Plexiglas is stuck to the upper side of its free end. The He–Ne 5 W Laser Micrometer irradiates the Plexiglas and reflects to a screen stuck on by a piece of coordinate paper in order to amplify the specimen deformation. A High Speed Video used at a frequency of 24 HZ records the process of movement of the light point during the process of laser irradiation. The television monitor connected with the video displays the movement of the light point recorded by High Speed Video. The principle of amplifying the specimen deformation by the Laser Micrometer is shown in Fig. 2. At the same time the Thermovision Infrared Camera records the real-time temperature distribution on the lateral area of the heated region, and is attached to a computer display.

The cross-section A–A of heated region center is cut and the sample is rapid cured resin as shown in Fig. 3. After polishing the sample, microstructure of the sample is shot by



Fig. 1. The scheme of the experiment.



$$y_1 = L_o \tan(90^\circ - \alpha')$$

$$y_2 = L_o \tan(90^\circ - \alpha' + \phi)$$

$$\phi = \tan^{-1}\left(\frac{\Delta y}{L_o} + \tan(90^\circ - \alpha')\right) - 90^\circ + \alpha'$$

Where: ϕ is the deformation angle; α is incidence angle; $\Delta y = y_2 - y_1$

Fig. 2. Conceptual diagram of amplifying specimen deformation.

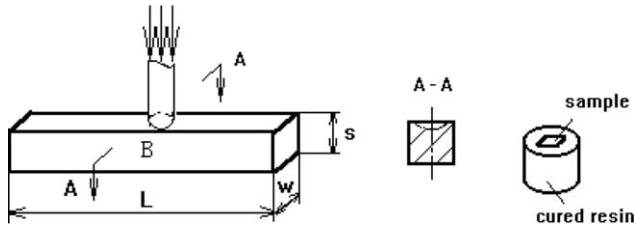


Fig. 3. The scheme of microstructure experiments.

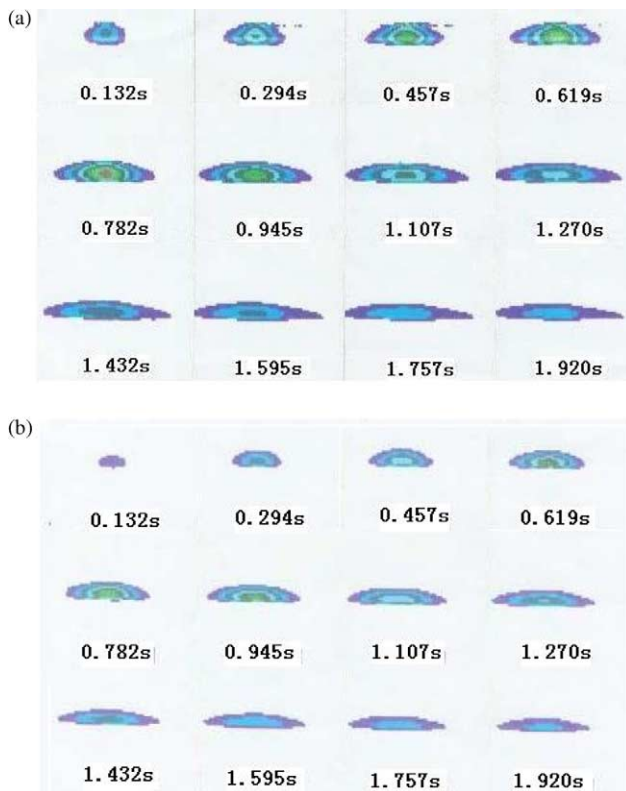


Fig. 4. The variation of the temperature distribution during the process of laser irradiation. (a) Material, St14; (b) Material, C45.

the NEOPHOT21 Metalloscope. Vickers Microhardness is measured along the central line of the cross-section A–A by Microhardness duro-meter. Hardness distribution curve is drawn.

2.2. Experimental results

During the process of laser irradiation the temperature distribution images on the lateral area of the heated region are shown in Fig. 4.

Fig. 4 shows that there is a kind of un-convention temperature distribution that the temperature of inner material is higher than that of the boundary in the limit thickness specimen under laser irradiation. It is thought that heat transfer in the limit thickness specimen possesses wave behavior different from diffusion.

Microstructure. After laser irradiation the microstructures of the cross-section heated region center are shown in Fig. 5. Hardness distribution curves in the specimen in thickness direction are shown in Fig. 6.

Because material St14 contains less carbon, Fig. 5(a) shows that there is the thinner heat affected region like the beginning of moon beneath surface, compositions are fined in it, Fig. 6(a) shows that hardness distribution curve in the specimen thickness direction changes a little. But material C45 contains more carbon, Fig. 5(b) shows that there is obvious transformation hardening region beneath surface. It is seen that the tiny martensite exists in the transformation region. Because of rapid cooling, the number of the retained austenite improves and the content of carbon in the austenite is restrained due to no time to diffuse. Therefore, the martensite transformed from this austenite contains higher carbon. Its hardness is improved 20% more than that of the conventional martensite. Hardness distribution curve in the specimen thickness direction changes notably as shown in Fig. 6(b).

Dynamic micro-deformation process. During the process of laser irradiation the variations of the dynamic micro-deformation versus time are shown in Fig. 7.

Fig. 7 indicates that when the laser beam irradiates on the specimen surface, the temperature on the upper surface in the heated region increases rapidly (not be exceeded melting point of material). Strong temperature gradient mainly occurs in the thickness direction of the specimen. Due to large thermal expansion and low yield stress on the upper surface under the high temperature, the material heated region produces compressive plastic deformation and causes material to accumulate. So the specimen deforms away from

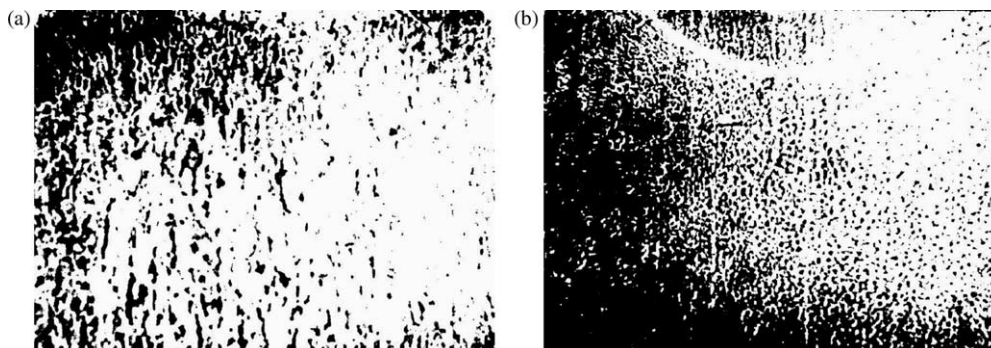


Fig. 5. Micrographs of the specimen after laser irradiation ($\times 40$). (a) Material, St14; (b) material, C45.

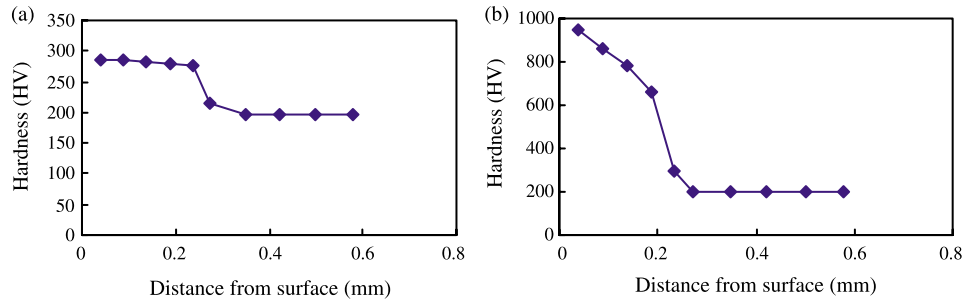


Fig. 6. Hardness distribution curve in the specimen thickness direction. (a) Material, St14; (b) material, C45.

the laser beam. With the continual heating time, the deformation is larger and larger, because heat transmits to the specimen in the form of wave, heat wave runs into limit boundary, it reflects and overlaps and makes temperature rise in the specimen interior. Its effect is to decrease the deformation and make the curve vary gently until a short time after the heating time finishes. The deformation angle depends on temperature gradient in the thickness direction and the geometry constraint of the specimen. After laser beam switches off, the temperature on the upper surface drops very quickly. Material contracts so that part of accumulative material recovers and compressive stress decreases. With the development of cooling process, due to heat conductance, the below layers of the specimen expand continually and elongate them. So the deformation away from laser beam reduces gradually, as far as the material C45 possesses phase transformation property, the martensitic transformation can cause volume expansion so that the deformation away from the laser beam increases. Therefore, the final deformation angle is the result of thermal deformation and phase transformation cooperation, the specimen made in material C45 is deformed away from the laser beam, but the specimen made in material St14 is deformed towards the laser beam.

3. Numerical simulation

3.1. Model of calculation

The specimen is discretized by means of 8-node linear brick elements to attain high precision because a steep

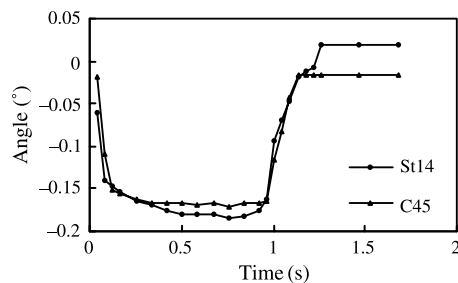


Fig. 7. The variation of the dynamic micro-deformation versus time during the process of laser interaction.

temperature gradient is produced in the heated region when laser beam irradiates on specimen surface. In order to improve efficiency and reduce calculation, there are dense meshes around the heated region and there are thin meshes away from heated region. In fact, the size of meshes is $0.2 \text{ mm} \times 0.2 \text{ mm} \times 0.2 \text{ mm}$ in heated region and meshes are thinner and thinner from around to away from the heated region. They are met the following formula

$$\frac{\kappa \Delta t}{\Delta x^2} \leq \frac{1}{2} \quad (1)$$

where κ is material thermo-diffused efficiency; Δt is time step; Δx is mesh size.

Meshes in FEM are shown in Fig. 8.

3.2. Boundary condition

Laser beam is input as a stream of heat flux vector in addition. The heat flux density distribution is regarded as obeying the Gauss distribution. The heat flux density away from the center of the laser spot is calculated with the following formula

$$q(r) = \frac{2AP}{\pi r^2} \exp\left(-\frac{2r^2}{r_b^2}\right) \quad (2)$$

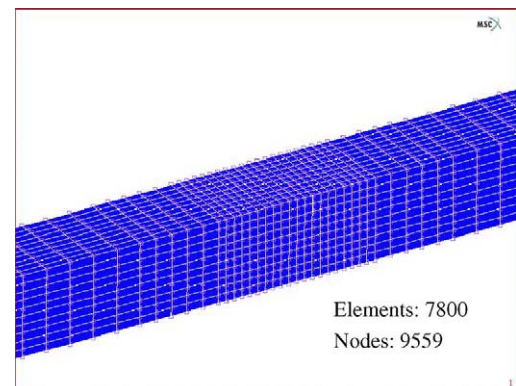


Fig. 8. FEM model of calculation.

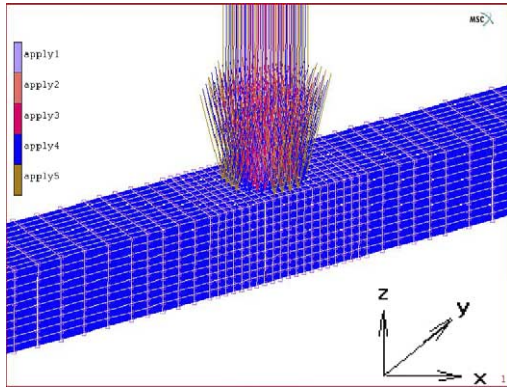


Fig. 9. The distribution levels of the thermal source energy density.

where A is the absorption coefficient of sheet metal ($A=0.45$); P is laser output power; r is the laser beam radius on the specimen surface; r_b is the distance from the center of the laser beam spot.

When the heating time is t , the heat energy absorbed by the specimen is described as:

$$Q = t \int_0^{r_b} 2\pi q(r)r dr \quad (3)$$

In calculated model, the distribution levels of the thermal source energy density are chosen as five in order to describe the laser beam spot as the circle shown in Fig. 9. Practice proved that this model could simulate actual situation. Calculated precision has been improved greatly.

The specimen cools in air after laser irradiation. β is regarded as total heat exchange coefficient including convection and radiation. The lost energy for heat exchange can be calculated with the following formula

$$q_h = \beta(T - T_0) \quad (4)$$

where T_0 is the room temperature in lab ($T_0=27.5\text{ }^\circ\text{C}$).

Value β is given to change versus temperature in steady condition [18]. According to cause deep temperature gradient in heated region after laser beam irradiated on the surface of sheet metal, value β is adjusted to 80–100 times of value in steady condition [19]. But we think that it is difficult to determine value β , because it not only increases with surface temperature gradient increasing, but

Table 1
Total heat exchange coefficient

Temperature (°C)	β [18] ($\text{W (m}^2 \text{K)}^{-1}$)	β [19] ($\text{W (m}^2 \text{K)}^{-1}$)	β ($\text{W (m}^2 \text{K)}^{-1}$)
20	6	480–600	90,000
300	50	4000–5000	59,000
600	120	9600–12,000	51,000
750	180	14,400–18,000	49,000
900	200	16,000–20,000	47,500
1200	250	20,000–25,000	42,000
1500	378	30,240–37,800	32,500

also depends on section size of specimen and cooling time. In order to simulate experimental results, we modify the value of β shown in Table 1.

3.3. Calculated process

The temperature distribution and dynamic micro-deformation process during the process of laser irradiation are numerically simulated by Msc.Marc software. Considering that the plastic deformation of specimen is caused by the thermal strain, while thermal strain is caused by the temperature distribution in the specimen. The traditional 3D transient analysis of the coupled thermal and mechanical interaction is adept in the process of calculation. The process of coupled calculation is shown in Fig. 10.

Thermo-physical properties of material depend on temperature shown in Fig. 11 [20].

Calculated technological parameters are chosen from experimental parameters. The subroutine of total heat exchange boundary condition is programmed by FORTRON language. Value β versus temperature is input by FILM user subroutine.

3.4. Calculated results

1. During the process of laser irradiation the temperature distribution images on the lateral area of the heated region are shown in Fig.12.
2. During the process of laser irradiation the variations of the dynamic micro-deformation versus time are shown in Fig. 13.

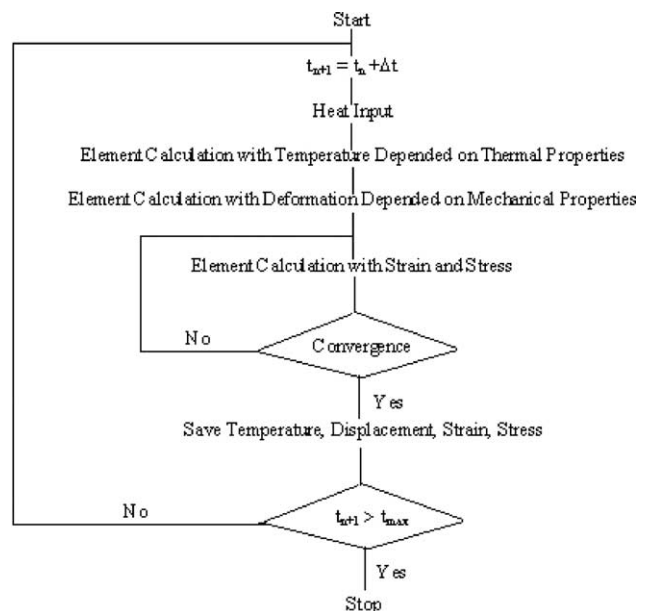


Fig. 10. The process of coupled calculation.

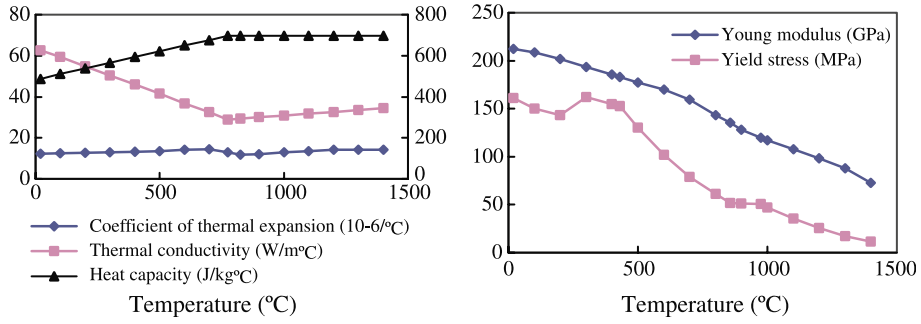


Fig. 11. The variation of thermal and mechanical properties of material versus temperature [20].

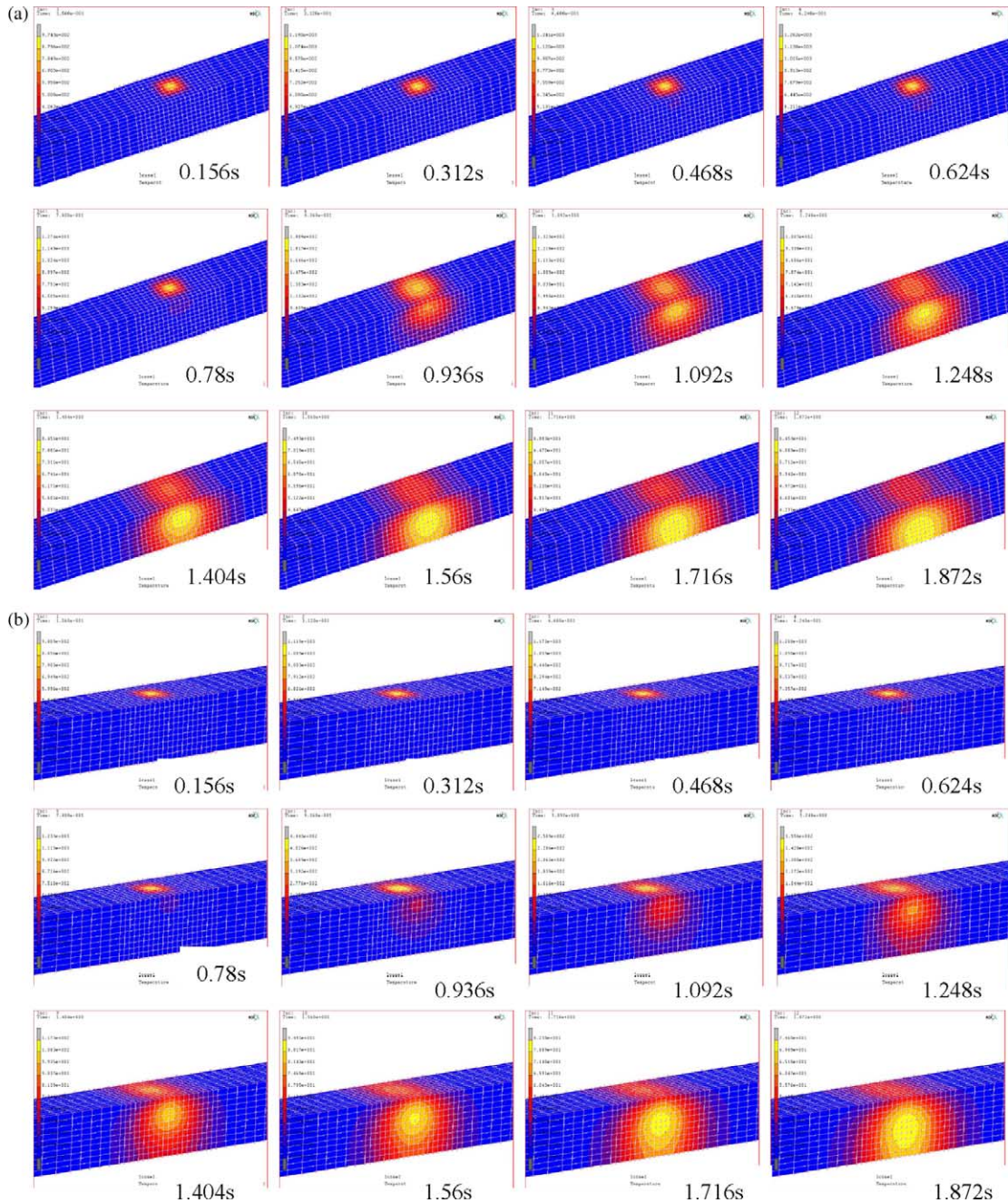


Fig. 12. The variation of the temperature distribution during the process of laser irradiation. (a) Material St14; (b) Material, C45.

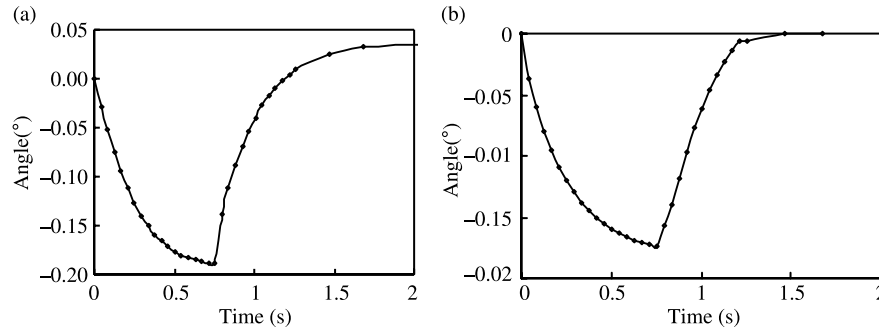


Fig. 13. The variation of the dynamic micro-deformation versus time during the process of laser interaction. (a) Material:St14; (b) material:C45.

4. Conclusion

Compared with experiment result and calculated result, the variation of the temperature distribution during the process of laser irradiation is the similitude, but the variation of the dynamic micro-deformation versus time is the difference. Although the largest deformation is almost the same, the deformation process is different. So the calculation of numerical simulation need be improved. The experiment phenomenon shows that heat transfers in the limit thickness specimen possesses wave behavior differs from diffusion. There is diffused wave overlapped by incident wave when the heat transfer in the specimen effected by reflected wave. The final result is that the temperature inside the specimen is higher than that of boundary. It seems that if the dynamic micro-deformation process of laser irradiation is described by wave theory, good calculated result to approach actual situation might be got.

According to experimental and calculated results, conclusion can be gained as follows:

- The final deformation direction of the specimen depends on the result of the thermal strain and the phase transformation strain cooperation, away from the laser beam or towards the laser beam. The final deformation angle depends on temperature gradient in the thickness direction and the geometry constraint of the specimen.
- It is not enough to simulate the dynamic micro-deformation of the specimen under laser point source through the model of calculation based on Fourier heat transfer theory.

Acknowledgements

The authors would like to acknowledge Andras Szilagyi, Dr Antal Sklanitz, Tamas Markovits and Zoltan Dudas for their assistance during the earlier stages of this work that was supported financially by China Scholarship Council and Hungary Ministry of Education, Natural Science Foundation of China, Aviation Fundamental Science Fund of China.

References

- [1] F. Vollertsen, Mechanisms and models for laser forming in: M. Geiger, F. Vollertsen (Eds.), Proceedings of the LANE'94, Meisenback, Bamberg, 1994, pp. 345–359.
- [2] F. Vollertsen, M. Rodle, Model for the temperature gradient mechanism of laser bending in: M. Geiger, F. Vollertsen (Eds.), Proceedings of the LANE'94, Meisenback, Bamberg, 1994, pp. 371–378.
- [3] X.F. Wang, J. Takacs, G. Krallics, et al., Research on the thermo-physical process of laser bending, Journal of Materials Processing Technology 127 (2002) 388–391.
- [4] X.F. Wang, Application of Laser Non-melting Processing Technology in the Sheet Metal Forming, Beijing University of Aeronautics and Astronautics, 2003. p. 1.
- [5] S. Holzer, H. Arnet, M. Geiger, Physical and numerical modelling of the bucking mechanism in: M. Geiger, F. Vollertsen (Eds.), Proceedings of the LANE'94, Meisenback, Bamberg, 1994, pp. 379–386.
- [6] J. Kraus, Basic processes in laser bending of extrusions using the upsetting mechanism, in: M. Geiger, F. Vollertsen (Eds.), Proceedings of the LANE'97 97, Meisenback, Bamberg, 1997, pp. 431–438.
- [7] N. Alberti, L. Fratini, F. Micari, Numerical simulation of the laser bending process by a coupled thermal mechanical analysis in: M. Geiger, F. Vollertsen (Eds.), Proceedings of the LANE'94, Meisenback, Bamberg, 1994, pp. 327–336.
- [8] P.J. Cheng, S.C. Lin, An analytical model of the temperature field in the laser forming of sheet metal, Journal of Materials Processing Technology 101 (2000) 260–267.
- [9] Y. Namba, Laser forming in space in: C.P. Wang (Ed.), International Conference on Laser'85 (1986), pp. 403–407.
- [10] M. Geiger, F. Vollertsen, G. Deinzer, Flexible straightening of car body shell by laser forming, SAE Paper No. 930279, 1993 pp. 354–361.
- [11] L. Weimin, M. Geiger, F. Vollertsen, Study on laser bending of metal sheets, Chinese Journal of Laser 25 (9) (1998) 859–864.
- [12] X.F. Wang, X.Y. Wang, D.S. Lin, Research on laser bending test of sheet metal, Metalforming Machinery 3 (1999) 8–10.
- [13] X.F. Wang, Effects on the sheet metal bending deformation of laser processing parameters, Aviation Engineering and Maintenance 4 (1999) 41–42.
- [14] J. Magee, K.G. Watkins, W.M. Steen, et al., Edge effects in laser forming in: M. Geiger, F. Vollertsen (Eds.), Proceedings of the LANE'97, Meisenback, Bamberg, 1997, pp. 399–408.
- [15] P.J. Cheng, S.C. Lin, Using neural networks to predict bending angle of sheet metal formed by laser, International Journal of Machine Tools and Manufacture 40 (2000) 1185–1197.

- [16] J. Lawtence, M.J.T. Schmidt, et al., The forming of mild steel plates with a 2.5 kW high power diode laser, *International Journal of Machine Tools and Manufacture* 41 (2001) 967–977.
- [17] K.C. Chan, Y. Harada, J. Liang, et al., Deformation behavior of chromium sheets in mechanical and laser bending, *Journal of Materials Processing Technology* 122 (2002) 272–277.
- [18] L. Shunhong, et al., Study on numerical of the temperature field in laser welding of steel sheet, *Welding Machine* 8 (2001) 16–19.
- [19] J. Eenqiu, *Transient Shock Effect of Heat Transfer, Mass Diffuse and Momentum Transfer*, Science Publisher, 1997. p. 2.
- [20] S. Amon, *Berührungsfreies Biegn mittels thermischer Spannungen*, Diplomarbeit am LFT, 1991.